Nanostructures

DOI: 10.1002/anie.200905542

Mismatch Strain versus Dangling Bonds: Formation of "Coin-Roll Nanowires" by Stacking Nanosheets**

*Aswani Yella, Enrico Mugnaioli, Martin Panthöfer, Ute Kolb, and Wolfgang Tremel**

Dedicated to Professor Dr. Arndt Simon on the occasion of his 70th birthday

Low-dimensional nanostructures, such as nanotubes or nanowires, have been of both fundamental and technological interest during the past two decades because of the intriguing electronic and physical properties that are intrinsically associated with the nanostructures' low dimensionality and quantum-confinement effects.[1] In particular, recent developments concerning 2D nanosheet crystals such as stable graphene[2] and layered transition-metal chalcogenides have triggered new discoveries in condensed-matter physics and electronics.[3] Further miniaturization of these 2D structures by lateral confinement can potentially lead to not only a modulation of electron-transport phenomena, but also enhanced reactivity and 2D host capabilities, which arise from the enlarged surface area and improved diffusion processes upon the intercalation of guest molecules.[4] The synthesis of such laterally confined 2D crystals, however, has remained a challenge as they are intrinsically unstable owing to a large number of peripheral dangling bonds.[5,6] As the strong bonding interactions occur within the layers and weak van der Waals interactions between the layers, layered materials prefer the formation of large 2D sheets with only few stacked layers, rather than a stack of small 2D sheets in a coin-roll fashion (Figure 1).

In the absence of external forces, the individual 2D sheets immediately roll up to form closed structures such as quasi-0D onion-like structures[7] or 1D tubes[8] in order to decrease the number of dangling bonds and the total energy of the system. In fact, graphene was presumed for a long time not to exist in the free state and was believed to be unstable with respect to other carbon compounds such as soot, fullerenes, and nanotubes.

Figure 1. Representation of the extended layers with a few stacked layers (left) and small layer segments with many stacked layers (right).

In a similar fashion, individual layers of chalcogenide layer-type phases are unstable toward bending and have a high propensity to roll into curved structures. Folding in the layered-transition-metal chalcogenides was recognized as early as 1979, which was well before the discovery of carbon nanotubes.[9] Raglike and tubular structures of MoS_2 were reported by Chianelli et al., who studied their application as hydrodesulfurization catalysts.[9] Ten years later, Divigalpitiya et al.[10] showed that single graphene-like sheets of molybdenum sulfide could be obtained by a process of exfoliation, and then restacked with organic molecules to obtain interesting hybrid materials with layered structures. Recently, Cheon and co-workers obtained 2D MoS_2 nanosheets by stabilizing the edges with surfactant molecules.[11] Helveg et al.[12] demonstrated that single-layered MoS_2 can be grown on a reconstructed Au(111) substrate. Atomic-resolution scanning tunneling microscopy was used to systematically map and classify the atomic-scale structure of triangular MoS_2 nanocrystals as a function of size.[13]

Herein, we describe an entirely new concept for the formation of stable, planar graphene-type metal(IV) chalcogenide sheets. The method is based on the stabilization of laterally confined (diameter ≈ 50 nm) nanosheet crystals by an internal force, structural strain, which prevents the formation of scroll structures[14] or nanotubes, and results in stacked coin-roll-type nanowires (CRNWs).

The first step in the synthesis of CRNWs is to control the 1D nano-object crystal structure by means of appropriate doping. As MS_2 (M = Nb, Mo, W, Re, Sn) nanotubes can be obtained by reductive sulfidization of the corresponding nanostructured oxides,[15] a potential strategy for the fabrication of "doped" MS_2 has to rely on the synthesis of "doped" metal oxide nanoparticles, either in a statistical or in an ordered (for example, core–shell-type) fashion.

[*] A. Yella, Dr. M. Panthöfer, Dr. U. Kolb, Prof. Dr. W. Tremel
Institut für Anorganische Chemie und Analytische Chemie
Johannes Gutenberg-Universität
Duesbergweg 10–14, 55099 Mainz (Germany)
Fax: (+49) 6131-39-25605
E-mail: tremel@uni-mainz.de
Dr. E. Mugnaioli
Institut für Physikalische Chemie, Johannes Gutenberg-Universität
Welderweg 11, 55099 Mainz (Germany)

[**] This work was supported by the Deutsche Forschungsgemeinschaft (DFG) within the priority program 1165 "Nanotubes and Nanowires: From Controlled Synthesis to Function". A.Y. is a recipient of a fellowship from POLYMAT, the Graduate School of Excellence of the State of Rhineland-Palatinate. We acknowledge the help of G. Glasser with the SEM and support from the Materials Science Center (MWFZ) in Mainz.

Supporting information for this article is available on the WWW under http://dx.doi.org/10.1002/anie.200905542.

The approach pursued here relies on core–shell nanowires with a Nb_2O_5 backbone and a $W_{18}O_{49}$ coating (experimental details are given in the Supporting Information). Niobium oxide nanowires (NWs) were obtained from a sol–gel process using ammonium niobium(V) oxalate as precursor, citric acid as the gel-forming agent, and hexadecylamine as a surfactant. The product consists of mostly well-separated niobium oxide NWs (lengths between 150 nm and 250 nm, diameters between 5 nm and 50 nm). Nb_2O_5 is the only crystalline phase, as shown by powder X-ray diffraction investigations (Figure S1 in the Supporting Information).

The TEM images in Figure 2a show that the NWs were not uniformly structured along the rod direction, but were aggregates of smaller particles. The aggregation of the particles to form wires may result from the structure-directing influence of the surfactant. After calcination (550 °C, 1 h), the particles formed larger aggregates (Figure 2b). The HRTEM images of the as-synthesized Nb_2O_5 NWs and after calcination (Figure S2 in the Supporting Information) reveal that all the rods grow along the *c* direction (Figure 2c). The lattice spacings indicate that the surfactant is not intercalated into the product in a manner observed for V_2O_5.[16]

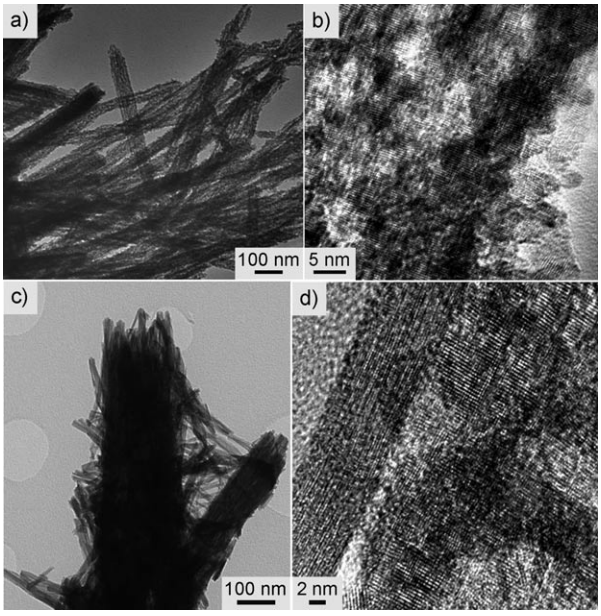

Figure 2. TEM and HRTEM images of the Nb_2O_5 and Nb_2O_5@$W_{18}O_{49}$ NWs. a) TEM image of the Nb_2O_5 NWs obtained after the sol–gel process and b) HRTEM image of a single NW obtained from the sol–gel process. c) After solvothermal treatment, the niobium oxide NWs were fully covered with tungsten oxide. d) HRTEM image of a niobium oxide NW partially covered with tungsten oxide.

In the next step, the as-obtained niobium oxide NWs were dispersed in ethanol. WCl_6 was added, and the mixture was sonicated for about 15 min to ensure that WCl_6 had completely dissolved. After solvothermal treatment of the mixture, the resulting blue precipitate was collected by filtration and washed with ethanol. The product $W_{18}O_{49}$ was identified from its X-ray powder diffraction patterns (Figure S3 in the Supporting Information). TEM images of the product (Figure 2c) show that the niobium oxide NWs were coated with tungsten oxide, so that the porous structure of the niobium oxide NWs no longer appeared, that is, some of the tungsten oxide may fill the pores of the niobium oxide NWs. An HRTEM image of the NWs is shown in Figure 2d, in which tungsten oxide indeed appears to be coated onto the niobium oxide NWs. Energy-dispersive X-ray spectroscopy (EDX) data revealed the presence of both tungsten and niobium in the NWs (Figure S4 in the Supporting Information).

The Nb_2O_5@$W_{18}O_{49}$ NWs were sulfidized in a reaction similar to that described in reference [15] by heating the coated NWs in Ar gas to 840 °C and subsequently passing a stream of H_2S through the vessel for 30 minutes. Conversion of the oxide to the sulfide took place in a similar manner to that described for pure WS_2 nanotubes, and resulted in the formation of Nb–W–S composite nanostructures. The product contains 1–8 μm long stacks of MS_2 platelets with diameters between 40 μm and 60 nm (Figure 3a, b); no MS_2 nanotubes were formed.

The X-ray powder diffraction pattern of the product (Figure 3c) shows that complete sulfidization occurred. Similarly, HRTEM and EDX analyses (Figure 3d) and STEM images of the nanostructures (Figure S5 in the Supporting Information) confirm the complete conversion of oxide NMs to sulfide CRNWs with an overall stoichiometry of $Nb_{1-x}W_{1-x}S_2$, with $x = 0.30$ (from EDX, 5% uncertainty).

Figure 3a further shows that the coin-roll NWs have a uniform morphology. HRTEM images clearly show these structures to be very different from the conventional curved nanostructures typically observed for layered chalcogenides, as the layers are stacked perpendicular to the growth direction of the chalcogenide nanotubes (Figure 3b). The interlayer spacing of 0.64 nm between the layers in the stacked NWs is slightly larger than the (002) *d* spacing of 2H-WS_2 and 2H-NbS_2.

Parallel platelet-like segments appear in an alternating periodic manner along the growth direction of the stacks, and the layers within the stacks are generally smooth. It is clear that the layers tend to bend between each segment on a length scale of about 5 nm. EDX spectra reveal the presence of both niobium and tungsten (Figure 3d).

In order to ascertain whether the stack formation is induced by a phase separation of WS_2 and NbS_2, or whether the stack is a quasi-binary $Nb_{1-x}W_xS_2$, additional line-scanning EDX analyses were performed. The results showed that both niobium and tungsten were present at each point along the line scan (Figure S6 in the Supporting Information). The CRNWs are not homogeneous in composition but are homogenous in morphology. Because of the mismatch strain, the CRNWs contain a mixture of tungsten-rich niobium sulfide and niobium-rich tungsten sulfide, which contain both niobium and tungsten at each point. These findings are consistent with strong deviations from Vegard's law of the bulk phases in the system NbS_2/MoS_2.[17] A closer view of the layers in the HRTEM image reveals diffuse bending and kinking that increase along the edges of the stacks (Figure 4b), while the whole structure remains straight.

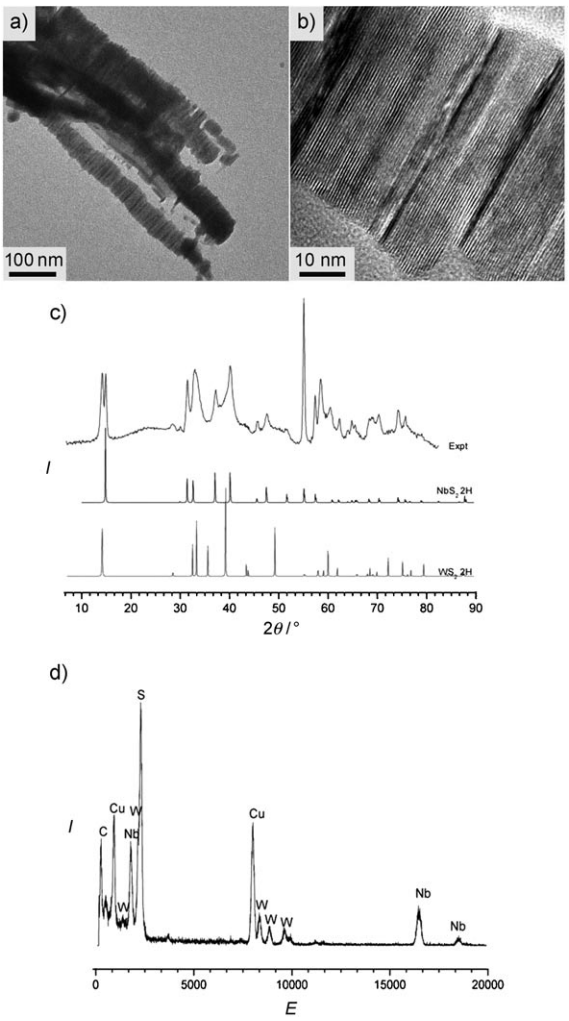

Figure 3. Characterization of the CRNWs. a) TEM image of the product obtained after sulfidization of the Nb_2O_5@$W_{18}O_{49}$ NWs. b) HRTEM image of the NWs. c) X-ray powder diffraction pattern. d) EDX analysis of the CRNWs.

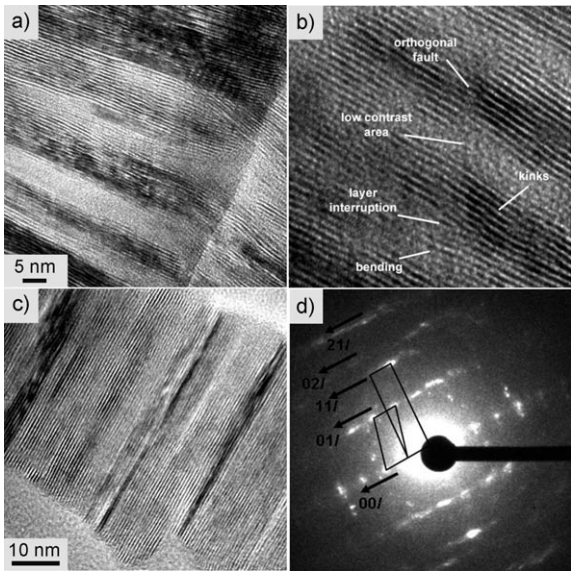

Figure 4. HRTEM images of the CRNWs. a, b) High-resolution images showing the curving of the layers along the segments. c) Periodic alternation along the stack. d) Corresponding electron diffraction pattern.

This result is surprising considering that kinks, interruption of layers, orthogonal faults, and low-contrast areas are observed.

The formation of all these defects can be related to the large compressive lateral lattice mismatch strain between NbS_2 and WS_2 during the crystal growth. Another indication of the presence of lattice strain is observable as a dark area in the TEM micrographs in between the 5 nm long segments (Figure 4c). Areas of low contrast show that the layers can bend orthogonal to the viewing direction, thus resulting in the loss of the Bragg conditions in HRTEM. The periodic contrast along the long axis of the CRNWs is due to the lattice distortion in $Nb_{1-x}W_xS_2$ and shows the presence of the strain field.

The nano-area electron diffraction (NED) pattern of the CRNWs presented in Figure 3d is shown in Figure 4d, and is the sum of the diffractions of different neighboring stacks. The 00*l** line is well-defined, thus indicating that n(001), that is, the normal-vector to lattice plane set in the (001) direction, is almost parallel for all the NW stacks. It is possible to observe distances between the Bragg maxima, which are consistent with a different orientation of a rhombohedral lattice in the orthogonal direction. This result suggests that the layers tend to pack in three-layer sequences and the stacks are free to rotate along the [001] direction.

The formation of the CRNWs from tungsten oxide coated niobium oxide NWs could be due to 1) the higher doping of tungsten in niobium sulfide, which does not allow the formation of the nanotube phase because of the mismatch strain or 2) the morphology of the original Nb_2O_5 NWs, which consist of smaller particles. The first conjecture is supported by supplementary experiments, which showed that the similar nanostructures of NbS_2 could not be prepared directly from Nb_2O_5 nanorods alone (Figure S7 in the Supporting Information). Therefore, the formation of CRNWs could be a mechanism to reduce interfacial or strain energy that originates from the interlamellar lattice mismatch between NbS_2 and WS_2.

We observed two pieces of evidence that the mismatch strain overcomes the energy of the dangling bonds. The first is a curving of the layers along the diameter of the NW, that is, perpendicular to the stacking normal direction (Figure 4a). In order to release the large strain energy that resulted from the formation of the disordered $Nb_{1-x}W_xS_2$ phase by doping of NbS_2 with WS_2, the individual sheets prefer stacking rather than scrolling to form an onion-like structure or a nanotube. It is possible to relieve strain by a compositional variation across the junction, thereby forming crystalline junctions without obvious structural defects. Therefore the junctions undergo structural relaxation during their growth to overcome the lattice mismatch by forming segments with different chemical compositions of $Nb_{1-x}W_xS_2$. An EDX line scan clearly demonstrates that both niobium and tungsten are present at each point of the stack, but with slight compositional

variations. The line scan is made clear by drawing the lines at each point. Depending on the length scale of the corresponding methods, the line scan is heterogeneous to XRD and homogenous to EDX. Because of a sizeable lattice mismatch between NbS_2 and WS_2, the effect of mismatch strain is particularly important. We note that the mismatch strain can increase the system energy when WS_2 is doped into the NbS_2 lattice. Therefore, composition and morphology have to be adapted accordingly to reduce the mismatch strain energy.

Lattice mismatch strain is widely used to control nanostructure formation. More than a decade ago, misfit layer compounds of the $(AQ)_n(MQ_2)_m$-type (A = Ca, Sr, Bi, Pb, Ba; M = Ti, Cr, Co, Nb,Ta, Rh; Q = O, S, Se) opened up a new vista on crystalline solids and stimulated an intense development of the superspace concept in modern crystallography.[18] In contrast with the asymmetric residual strain arising from the lattice mismatch between NbS_2 and WS_2 in the $Nb_{1-x}W_xS_2$ CRNWs, the structural strain in this class of compounds results from the misfit of the in layer translation periods of the NaCl-like AQ and the MoS_2-like MQ_2 sheets.

The majority of the product contains twinned nanostacks with a zigzag surface morphology, as evident from the scanning electron microscopy (SEM) images in Figure 5. The high-resolution SEM image (Figure 5a) clearly shows that the cross section of these nanostacks consists of stacked hexagonal platelets. The zigzag morphology of the NW can result from a stacking of oblique hexagonal platelets (Figure 5b).

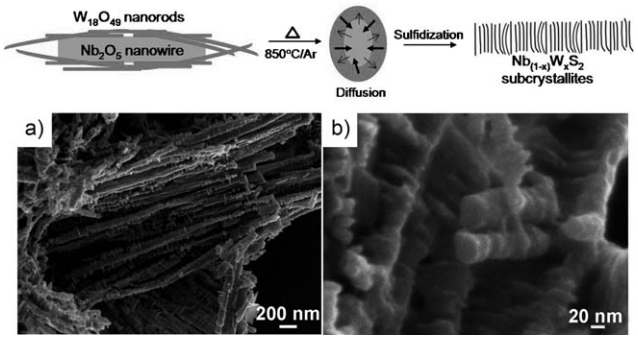

Figure 5. Top: Formation of the CRNWs: Nb_2O_5 NW coated with $W_{18}O_{49}$. Left: Cross-section of a core-shell NW illustrating the balancing of the Nb/W concentration gradient by diffusion of W atoms from the $W_{18}O_{49}$ shell into the Nb_2O_5 core and vice versa. Right: Formation of a $Nb_{(1-x)}W_xS_2$ stacked CRNW from grains with different orientations upon sulfidization of the oxide NW. The formation of the CRNWs is completed with new $Nb_{(1-x)}W_xS_2$ grains growing in the limited space between two large grains. a) SEM image of the stacked NWs in a horizontal view and b) in a vertical view showing the kinks.

The NWs described here are composed of both niobium and tungsten disulfide, similar to the niobium-doped tungsten sulfide tubes reported by Walton and co-workers.[19] This composition may be attributed to the diffusion of tungsten atoms into the niobium oxide nanorods upon heating to 850 °C. As a result, W atoms may occupy some of the Nb positions within the Nb_2O_5 NWs or occupy the empty sites at the grain boundaries between the particles in the NWs, thus leading to the formation of a ternary $W_xNb_yO_z$ phase.

We have also observed other intriguing structures such as a nanotube backbone coated with whiskers (Figure 6) upon increasing the volume fraction of the tungsten oxide shell. In

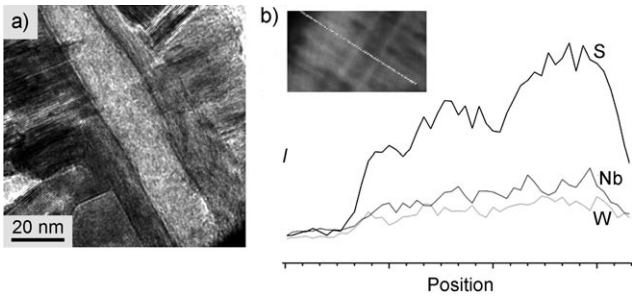

Figure 6. Characterization of branched nanotubes. a) HRTEM image of a nanotube obtained from niobium oxide NWs coated with excess tungsten oxide. After sulfidization, the core–shell NW phase segregated into tungsten-rich nanotubes decorated with the ternary $Nb_{1-x}W_xS_2$ sheets. b) EDX line-scan analysis of a sheet-decorated nanotube. The inset shows the corresponding area on which the EDX line scan was performed.

this case, it appears that the outer hexagonal platelets grow on top of an inner multiwall nanotube. An EDX analysis of the nanotube backbone coated with whiskers revealed the presence of both niobium and tungsten. As this whisker-decorated tube was generated from a niobium oxide backbone coated with tungsten oxide, one might expect the backbone to consist of NbS_2 with WS_2 sheets attached. Surprisingly, however, the EDX line scan analysis shows that the tube is tungsten-rich whereas the sheets have a composition of $Nb_{0.67}W_{0.33}S_2$. In particular, niobium oxide NWs coated with high amounts of tungsten oxide were observed to form an oxide with higher tungsten content when heated to 850 °C, which, after sulfidization, phase-segregated into tungsten-rich nanotubes decorated with sheets of the ternary $Nb_{1-x}W_xS_2$ phase. These results confirm that the metal oxide that forms the shell component plays a key role in the formation of the stacked nanostructures as summarized by Equations (1) and (2):

$$Nb_2O_5\,(\text{nanorod}) + WO_x\,(\text{coating}) \rightarrow Nb_xW_yO_z\,(\text{nanorod}) \quad (1)$$

$$Nb_xW_yO_z\,(\text{nanorod}) + H_2S\,(\text{gas}) \rightarrow Nb_{0.7}W_{0.3}S_2\,(\text{coin-roll nanowire}) + H_2O\,(\text{gas}) \quad (2)$$

Hence, the stacked NWs may be formed as a result of oxide–sulfide template conversion in order to minimize the strain energy that results from lateral lattice mismatch.

In conclusion, we have demonstrated the formation of stacked CRNWs of layered metal chalcogenides by "doping". The presence of internal strain leads to substitution of approximately 30% of niobium by tungsten and the formation of stacked NWs rather than Nb doped $Nb_{1-x}W_xS_2$ nanotubes. For higher substitution levels of tungsten into

the niobium (ca. 50%), tungsten-rich $W_{1-x}Nb_xS_2$ nanotube backbones decorated with niobium-rich $Nb_{1-x}W_xS_2$ sheets were formed. This result suggests that mixed niobium–tungsten oxides form the basis for very different types of stacked nanostructures which, because of short diffusion pathways for potential intercalants, may find various applications for example, in lithium ion batteries. The intercalation and deintercalation of lithium ions, which is currently under investigation, is expected to be easier and faster in the case of the stacked NWs compared to conventional nanotubes, fullerenes, or bulk structures. Furthermore, the large surface area and the large number of exposed edge atoms may lead to high activities of these materials in heterogeneous catalysis.

Received: October 4, 2009
Revised: January 25, 2010
Published online: March 12, 2010

Keywords: metal chalcogenides · nanotubes · nanowires · niobium sulfide · tungsten sulfide

[1] G. A. Ozin, A. C. Arsenault, L. Cademartiri, *Nanochemistry: A Chemical Approach to Nanomaterials*, The Royal Society of Chemistry, Cambridge, 2nd ed., **2008**.
[2] A. K. Geim, K. S. Novoselov, *Nat. Mater.* **2007**, *6*, 183–191.
[3] K. S. Novoselov, A. K. Geim, S. V. Morozov, D. Jiang, Y. Zhang, S. V. Dubonos, I. V. Grigorieva, A. A. Firsov, *Science* **2004**, *306*, 666–669.
[4] *Intercalated Layered Materials* (Ed.: F. A. Levy), Kluwer Academic Publishers, Dordrecht, **1979** (Physics and Chemistry of Materials with Layered Structures Series).
[5] a) W. Tremel, *Angew. Chem.* **1999**, *111*, 2311–2315; *Angew. Chem. Int. Ed.* **1999**, *38*, 2175–2179; b) R. Tenne, *Nat. Nanotechnol.* **2006**, *1*, 103–111.
[6] a) J. Zhang, J. M. Soon, K. P. Loh, J. Yin, J. Ding, M. B. Sullivan, P. Wu, *Nano Lett.* **2007**, *7*, 2370–2376; b) A. Vojvodic, B. Hinnemann, J. K. Nørskov, *Phys. Rev. B* **2009**, *80*, 125416.
[7] L. Margulis, G. Salitra, R. Tenne, M. Talianker, *Nature* **1993**, *365*, 113–114.
[8] Y. Feldman, E. Wasserman, D. J. Srolovitz, R. Tenne, *Science* **1995**, *267*, 222–225.
[9] R. R. Chianelli, E. Prestridge, T. Pecorano, J. P. DeNeufville, *Science* **1979**, *203*, 1105–1107.
[10] W. M. R. Divigalpitiya, R. F. Frindt, S. R. Morrison, *Science* **1989**, *246*, 369–371.
[11] J.-W. Seo, Y.-W. Jun, S. W. Park, H. Nah, T. Moon, B. Park, J.-G. Kim, Y. J. Kim, J. Cheon, *Angew. Chem.* **2007**, *119*, 8984–8987; *Angew. Chem. Int. Ed.* **2007**, *46*, 8828–8831.
[12] S. Helveg, J. V. Lauritsen, E. Lægsgaard, I. Stensgaard, J. K. Nørskov, B. S. Clausen, H. Topsøe, F. Besenbacher, *Phys. Rev. Lett.* **2000**, *84*, 951–954.
[13] J. V. Lauritsen, J. Kibsgaard, S. Helveg, H. Topsøe, B. S. Clausen, E. Lægsgaard, F. Besenbacher, *Nat. Nanotechnol.* **2007**, *2*, 53–58.
[14] O. G. Schmidt, K. Eberl, *Nature* **2001**, *410*, 168.
[15] a) A. Rothschild, J. Sloan, R. Tenne, *J. Am. Chem. Soc.* **2000**, *122*, 5169–5179; b) H. A. Therese, J. Li, U. Kolb, W. Tremel, *Solid State Sci.* **2005**, *7*, 67–72; c) H. A. Therese, N. Zink, U. Kolb, W. Tremel, *Solid State Sci.* **2006**, *8*, 1133–1137.
[16] H. A. Therese, F. Rocker, A. Reiber, J. Li, M. Stepputat, G. Glasser, U. Kolb, W. Tremel, *Angew. Chem.* **2005**, *117*, 267–270; *Angew. Chem. Int. Ed.* **2005**, *44*, 262–265.
[17] U. Hotje, M. Binnewies, *Z. Anorg. Allg. Chem.* **2005**, *631*, 2467–2474.
[18] G. A. Wiegers, *Prog. Solid State Chem.* **1996**, *24*, 1–139.
[19] Y. Q. Zhu, W. K. Hsu, S. Firth, M. Terrones, R. J. H. Clark, H. W. Kroto, D. R. Walton, *Chem. Phys. Lett.* **2001**, *342*, 15–21.

